Thermoelectric transport through a quantum dot with a magnetic impurity*

Yu Zhen(于 震)[a], Guo Yu (郭 宇)[b], Zheng Jun(郑 军)[a)c)], and Chi Feng(迟 锋)[b)†]

[a)] College of Engineering, Bohai University, Jinzhou 121013, China
[b)] School of Mathematics and Physics, Bohai University, Jinzhou 121013, China
[c)] State Key Laboratory of Superlattices and Microstructures, Institute of Semiconductors, Chinese Academy of Sciences, Beijing 100083, China

(Received 7 April 2013; revised manuscript received 24 May 2013)

We study the thermoelectric effect in a small quantum dot with a magnetic impurity in the Coulomb blockade regime. The electrical conductance, thermal conductance, thermopower, and the thermoelectrical figure of merit (FOM) are calculated by using Green's function method. It is found that the peaks in the electrical conductance are split by the exchange coupling between the electron entering into the dot and the magnetic impurity inside the dot, accompanied by the decrease in the height of peaks. As a result, the resonances in the thermoelectric quantities, such as the thermal conductance, thermopower, and the FOM, are all split, opening some effective new working regions. Despite of the significant reduction in the height of the electrical conductance peaks induced by the exchange coupling, the values of the FOM and the thermopower can be as large as those in the case of zero exchange coupling. We also find that the thermoelectric efficiency, characterized by the magnitude of the FOM, can be enhanced by adjusting the left–right asymmetry of the electrode–dot coupling or by optimizing the system's temperature.

Keywords: quantum dot, thermoelectric effect, magnetic impurity

PACS: 73.21.La, 72.15.Jf, 73.50.Lw **DOI:** 10.1088/1674-1056/22/11/117303

1. Introduction

With some recent experimental[1–5] and theoretical[6–9] breakthroughs, the thermoelectric effect in low-dimensional mesoscopic systems has attracted much interest due to the high efficiency of converting heat into electricity, or vice versa. The efficiency of thermoelectrical materials in the linear response regime where the gradients of both the temperature and electric fields are infinitely small is described by the thermoelectrical figure of merit (FOM) ZT whose expression is $ZT = GS^2T/\kappa$, where G is the electrical conductance, S the thermopower (or Seebeck coefficient) determined by subtracting the ratio between the electric energy eV (V is the bias voltage across the left and right electrodes) induced by the temperature difference ΔT in the absence of charge current T, i.e., $S = -\frac{eV}{\Delta T}|_{I=0}$. The thermal conductance κ is contributed by both the electrical and the phonon ones. In conventional bulk thermoelectrical materials, the ratio κ/GT remains constant according to the Wiedmann–Franz law,[10] which has been broken since 2001 in nanoscale structures.[1–5] To be specific, the magnitude of the thermopower in such structures is significantly enhanced by the sharp features of the electronic density of states (DOS) resulted from the quantum size effect. Moreover, the heat flow carried by the phonons or the phonon thermal conductance can be reduced by particular device design with the help of the phonon engineering technique.[11,12] Much work has been devoted to the research subject in pursuit of large FOM values in various low-dimensional systems. As a zero-dimensional quantum structure, the quantum dot (QD) has become an extensively studied object due to the existence of discrete energy levels and tunable Coulomb interaction between electrons,[6,13–25] which can all lead to sharp features of the DOS and to the violation of the Wiedmann–Franz law.[26]

In recent years, some researchers have studied the thermoelectric phenomena in a QD structure modulated by the Fano[27–32] and Kondo[33–35] effects, which are characterized by the peaked configuration of the DOS or the electrical conductance. Essentially, these two effects arise from the strong correlation between the electrons in the dot and those in the electrodes connected to the dot. In addition, recent experimental[36] and theoretical[37] work has indicated that discrete energy levels can be induced by intra-dot magnetic exchange interactions (between electrons and the magnetic impurity in the dot). In most cases, the magnetic impurity is modeled by another QD with odd occupancy, but it can also be a transitional magnetic atom (Co), as used in a recent experiment,[36] in which an electron entering QD will form with the magnetic impurity a singlet or a triplet state. The kind of the formed state depends on the sign of the exchange coupling strength between the electron and the impurity. Additional resonances then emerge when the dot energy level aligns with these states, indicating the formation of sharp features of the DOS which will play an important role in the thermoelectrical performance. To the best of our knowledge,

*Project supported by the National Natural Science Foundation of China (Grant No. 61274101) and the SKLSM (Grant No. CHJG200901).
†Corresponding author. E-mail: chifeng@semi.ac.cn
© 2013 Chinese Physical Society and IOP Publishing Ltd

this issue has never been addressed and becomes the motivation of the present paper. As shown in Fig. 1, we study the thermoelectric performance of a QD that contains a magnetic impurity. The left and right electrodes are respectively held at temperatures of $T_{\rm L}$ and $T_{\rm R}$ with chemical potentials of $\mu_{\rm L}$ and $\mu_{\rm R}$. As will be shown later, the peaks in the electrical conductance that are originally positioned at the dot levels of $\varepsilon_{\rm d}=\mu$ and $\varepsilon_{\rm d}=-U+\mu$, where $\mu=\mu_{\rm L}=\mu_{\rm R}$ is the equilibrium chemical potential in the electrodes, are all split into two by the exchange interaction between the transporting electrons and the impurity. Meanwhile, the heights of the peaks are all obviously lowered. Interestingly, the strengths of the thermopower and the FOM can now be unchanged or slightly weakened, opening up some effective new working regions.

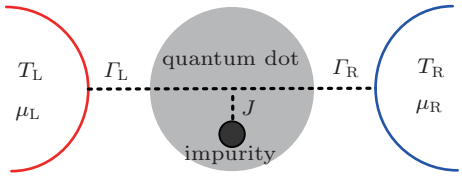


Fig. 1. (color online) Schematic picture of a quantum dot connected to the left and right electrodes with coupling strengths of $\Gamma_{\rm L}$ and $\Gamma_{\rm R}$. The two electrodes are individually held at temperatures of $T_{\rm L}$ and $T_{\rm R}$, and their chemical potentials are $\mu_{\rm L}$ and $\mu_{\rm R}$, respectively. Electrons transporting through the quantum dot interact with a magnetic impurity through an exchange coupling J.

2. Model and method

The Hamiltonian for the whole system is described by the Anderson model,[37,38]

$$H = \sum_{k,\sigma,\beta}\varepsilon_{k\beta}c^{\dagger}_{k\beta\sigma}c_{k\beta\sigma}+\varepsilon_{\rm d}\sum_{\sigma}d^{\dagger}_{\sigma}d_{\sigma}+Ud^{\dagger}_{\uparrow}d_{\uparrow}d^{\dagger}_{\downarrow}d_{\downarrow} + \sum_{k,\sigma,\beta}(V_{\beta{\rm d}}c^{\dagger}_{k\beta\sigma}d_{\sigma}+{\rm H.c.})+J\boldsymbol{s}\cdot\boldsymbol{S}, \quad (1)$$

where $c^{\dagger}_{k\beta\sigma}$ ($c_{k\beta\sigma}$) is the creation (annihilation) operator of the electrons with momentum k, spin σ, and energy $\varepsilon_{k\beta}$ in the β ($={\rm L},{\rm R}$) electrode; $d^{\dagger}_{\sigma}$ (d_{σ}) creates (annihilates) an electron with spin σ and energy $\varepsilon_{\rm d}$ in the QD with U being the intra-dot Coulomb interaction between the electrons. The fourth term on the right-hand side of Eq. (1) represents the dot–electrode coupling with strength of $V_{\beta{\rm d}}$. The last term in Eq. (1) stands for the exchange interaction between the electrons entering the QD and the unpaired spin on the magnetic impurity. We emphasize that this correlation originates from the exchange coupling between the electrical Coulomb interaction but not the direct coupling between the spin magnetic momentums of the electrons. Here, $\boldsymbol{s}$ and $\boldsymbol{S}$ are respectively the spin operators for the electrons at level $\varepsilon_{\rm d}$ and the magnetic impurity. By imposing single occupancy at the impurity $c^{\dagger}_{0\uparrow}c_{0\uparrow}+c^{\dagger}_{0\downarrow}c_{0\downarrow}=1$ and $S=\hat{\sigma}/2$, where $c^{\dagger}_{0\sigma}(c_{0\sigma})$ is the creation (annihilation) operator of the electrons on the magnetic impurity, we arrive at $c^{\dagger}_{0\uparrow(\downarrow)}c_{0\uparrow(\downarrow)}=(1\pm\hat{\sigma}_z)/2$, $c^{\dagger}_{0\uparrow}c_{0\downarrow}=\hat{\sigma}^{+}/2$, and $c^{\dagger}_{0\downarrow}c_{0\uparrow}=\hat{\sigma}^{-}/2$, where $\hat{\sigma}^{+(-)}=\hat{\sigma}_x\pm{\rm i}\hat{\sigma}_y$ and $\hat{\sigma}=(\hat{\sigma}_x,\hat{\sigma}_y,\hat{\sigma}_z)$ are the Pauli matrices. The exchange coupling Hamiltonian can then be written as[37,38]

$$J\boldsymbol{s}\cdot\boldsymbol{S} = \frac{J}{2}\sum_{\sigma,\sigma'=\uparrow,\downarrow}d^{\dagger}_{\sigma}d_{\sigma'}c^{\dagger}_{0\sigma'}c_{0\sigma} = \frac{J}{2}(n_{\uparrow}-n_{\downarrow})S^{z}+\frac{J}{2}d^{\dagger}_{\uparrow}d_{\downarrow}S^{-}+\frac{J}{2}d^{\dagger}_{\downarrow}d_{\uparrow}S^{+}, \quad (2)$$

where a constant term $J/2$ is neglected.

The electric and heat currents can be derived by Keldysh Green's function technique as[24]

$$\begin{pmatrix}J_{\rm e}\\ Q\end{pmatrix}=\frac{1}{h}\int{\rm d}\varepsilon\begin{pmatrix}-e\\ \varepsilon-\mu\end{pmatrix}[f_{\rm L}(\varepsilon)-f_{\rm R}(\varepsilon)]T(\varepsilon), \quad (3)$$

where $f_{\beta}(\varepsilon)=\{1+{\rm e}^{(\varepsilon-\mu_{\beta})/k_{\rm B}T_{\beta}}\}^{-1}$ is the Fermi distribution function of lead β with chemical potential μ_{β}, temperature T, and Boltzmann constant $k_{\rm B}$. As we are interested in the linear-response regime, the chemical potentials and the temperatures of the two leads are set to be $\mu_{\rm L}=\mu_{\rm R}=\mu$ and $T_{\rm L}=T_{\rm R}=T$. The transmission coefficient $T(\varepsilon)$ can be expressed in terms of Green's function as[24]

$$T(\varepsilon)={\rm i}\sum_{\sigma}\frac{\Gamma_{\rm L}\Gamma_{\rm R}}{\Gamma_{\rm L}+\Gamma_{\rm R}}[G^{r}_{\sigma}(\varepsilon)-G^{a}_{\sigma}(\varepsilon)], \quad (4)$$

where $G^{r(a)}_{\sigma}(\varepsilon)$ and $\Gamma_{\beta}=2\pi\sum_{k}|V_{\beta d}|^{2}\delta(\varepsilon-\varepsilon_{k\beta})$ are QD' retarded (advanced) Green's function and the line-width function, respectively. We calculate Green's function by using the equation of motion method, which was given explicitly in Refs. [37] and [38]. Once Green's functions are obtained, we can calculate the thermoelectric quantities by[16,24]

$$G=\frac{e^{2}}{h}K_{0}(\mu,T), \quad (5)$$

$$S=-\frac{1}{|e|}\frac{K_{1}(\mu,T)}{K_{0}(\mu,T)}, \quad (6)$$

$$\kappa=\frac{1}{h}\left[K_{1}(\mu,T)eS+\frac{K_{2}(\mu,T)}{T}\right], \quad (7)$$

where $K_{n}(\mu,T)=\int{\rm d}\varepsilon(-\partial f(\varepsilon)/\partial\varepsilon)(\varepsilon-\mu)^{n}T(\varepsilon)$ with $n=0,1,\ldots$ and $f(\varepsilon)=\{1+{\rm e}^{(\varepsilon-\mu)/k_{\rm B}T}\}^{-1}$. In low temperatures, the contribution from the lattice vibration (phonon) to the thermal conductance can be approximated by $\kappa_{\rm ph}=\pi^{2}k_{\rm B}^{2}T/(3h)$.[39] Here we neglect this term since the transport of phonon can be blocked by using a particular device design.[11,12,16]

3. Numerical results

In the following numerical calculations, we choose the intra-dot Coulomb interaction $U=1$ as the energy unit and set the constants $e=\hbar=k_{\rm B}=1$. The equilibrium chemical potentials of the two electrodes are set to be $\mu_{\rm L}=\mu_{\rm R}=\mu=0$. Figure 2 shows the electrical conductance G, thermal conductance κ, thermopower S, and ZT versus the dot level $\varepsilon_{\rm d}$ under the condition of $\Gamma_{\rm L}=\Gamma_{\rm R}=0.02U$ and different values of

the exchange coupling strength J. When the QD is free from the magnetic impurity ($J = 0$), both the electrical conductance in Fig. 2(a) and the thermal conductance in Fig. 2(b) have two well-defined peaks positioned respectively around $\varepsilon_d = 0$ and $\varepsilon_d = -U$.[22,24] The peaks of the thermal conductance are wider than those of the electrical conductance, and the separation between them is also larger than those of the electrical one. This is because the thermal conductance depends on both electrical conductance and heat carried by each electron, and then has wider peaks around the conducting channels in the energy space.[22,24,39] The thermopower S has three zero points individually centered at $\varepsilon_d = -U$, $-U/2$, and 0. Across these zero points, the thermopower changes sign due to the electron–hole symmetry. Taking the $\varepsilon_d = 0$ conducting channel as an example, the detailed reason for the behavior of the thermopower can be explained as follows.[22,24] When the dot level ε_d is above the channel which is aligned with the chemical potential in the lead μ, there are more electrons excited by the temperature gradient from which the thermoelectric effect originates. Then, a voltage drop is generated when the electrons transport from the hotter left lead to the colder right lead under the open circuit (zero charge current) condition, resulting in negative thermopower as in units of k_B/e. When ε_d is aligned to the chemical potential $\mu = 0$, the thermopower vanishes since an equal number of electrons and holes are tunneling in the same direction, or equal numbers of electrons are flowing in opposite directions, and then the charge current is cancelled out. When ε_d is below the channel, the main carriers become the holes (or electrons are tunneling from the right electrode to the left) and then the thermopower changes sign.

As shown by the black solid line in Fig. 2(d), the FOM for $J = 0$ has two peaks positioned respectively at the left and right sides of the two channels $\varepsilon_d = 0$ and $\varepsilon_d = -U$, which is determined by the combined effect of the quantities discussed above, i.e., G, κ, and S. It has three zero points at $\varepsilon_d = 0$, $-U/2$ (the electron–hole symmetry point), and $-U$, where the thermopower $S = 0$. The four maxima are much larger than 1, indicating the violation of the Wiedmann–Franz law. This originates from the sharp features of the DOS of the QD indicated by the electrical conductance. In the presence of the exchange interaction between the electrons entering into the QD and the magnetic impurity inside the dot, the original two peaks in the electrical conductance are individually split into two (see Fig. 2(a)). This is because the spin unpaired electron on the magnetic impurity forms with the transporting electron singlet and triplet states whose state energies are respectively $3J/4$, $-J/4$, $-U + J/4$, and $-U - 3J/4$.[37,38] As shown in Fig. 2(a), the four peaks for the case of $J > 0$ are well defined whereas those for the case of $J < 0$, the peaks at $\varepsilon_d = 3J/4$ and $-U - 3J/4$, which are the excited states, are quite small. The reason is that the channel of the ground state is more favorable for electron transportation than the excited state.[37,38] Accordingly, higher peaks originate from electrons transporting through the ground states, which are singlet $3J/4$ and $-U - 3J/4$ for positive J, whereas triplet $|J|/4$ and $-U - |J|/4$ for negative J. Moreover, transport through the threefold degenerate triplet state is favored as compared with the nondegenerate singlet state. Note that the energy levels at $3J/4$ and $-U - 3J/4$ for $J < 0$ are singlet excited states, and this is why the peaks there are very small. The thermal conductance κ in Fig. 2(b) resembles the behavior of the electrical conductance, except that the widths of the peaks are broadened.

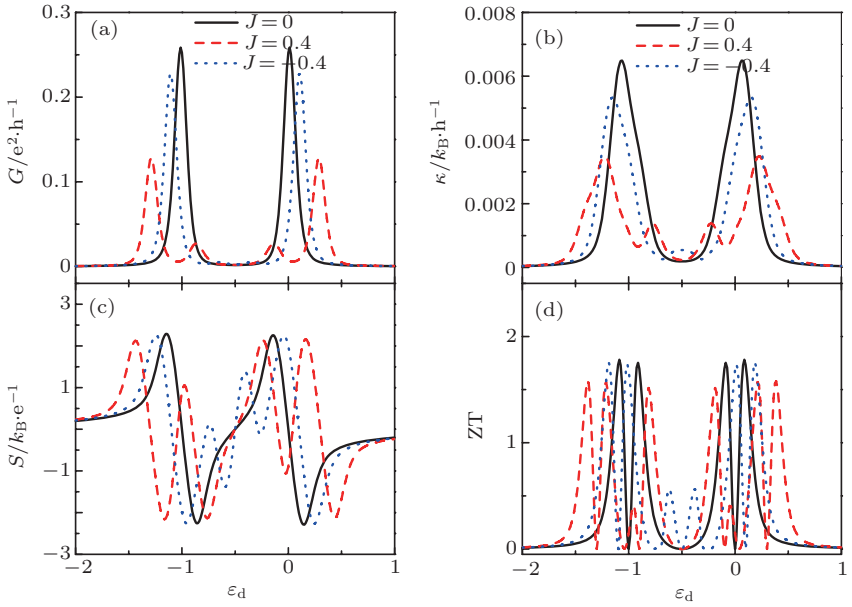


Fig. 2. (color online) (a) Linear electrical conductance G, (b) thermal conductance κ, (c) thermal power S, and (c) figure of merit ZT as functions of the dot level ε_d with different values of exchange coupling J. Other parameters are $\Gamma_L = \Gamma_R = 0.02$, and $T = 0.03$.

For the thermopower given in Fig. 2(c) in the case of $J \neq 0$, there are two points are worth pointing out. Firstly, similar to the case of $J = 0$, the thermopower now has two well defined peaks positioned individually at the left and right sides of each resonance in the electrical conductance. The two main twin peaks at states of $3J/4$ and $-U - 3J/4$ are still antisymmetric with respect to the $S = 0$ point, but the height of the negative and positive maxima of the other two at states of $-J/4$ and $-U + J/4$ are not equal to each other. We attribute this difference to the behavior of the thermal conductance in Fig. 2(b) induced by the excited states. For $J < 0$, the peaks in the thermopower are more clear than those in the electrical and thermal conductances. Secondly, although the peaks' height of the electrical and thermal conductances in the presence of magnetic impurity is much lower than the case of $J = 0$, the height of the main peaks around the ground states in the thermopower can be as large as those for $J = 0$. We think this is quite favorable in the thermoelectric effect, since large voltage drop is generated with small electrical and thermal conductances. Moreover, the heights of the peaks resulting from other molecular states are also quite high in spite of small electrical and thermal conductances, opening some promising work regions for thermoelectric designs. Behaviors of the FOM in Fig. 2(d) resemble that of the thermopower with quite large values of the peaks' height. It shows that the twin peaks in the FOM resulting from the excited states are relatively low due to the property of the thermopower.

Similar to the electronic transport through nanoscale devices, thermoelectric transport is sensitive to the system's symmetry.[15,16,25,40] In Fig. 3 we present the physical quantities varying with respect to the QD level for different values of the dot–electrode coupling asymmetry factor $\lambda = \Gamma_R/\Gamma_L$. The electrical and thermal conductances in Figs. 3(a) and 3(b) are significantly suppressed by increasing the left–right asymmetry (decreasing λ). The thermopower in Fig. 3(c), however, seems to be less influenced by the left–right coupling asymmetry, which is consistent with the conclusion drawn in Ref. [40]. Since the thermal conductance is determined by both the transmission coefficient (characterized by the electrical conductance) and the heat energy carried by the electrons, decrease in λ imposes great impact on the thermal conductance, leading to more significant suppression than the electrical conductance. As a result, the FOM in Fig. 3(d) can be enhanced, which is consistent with our previous results in Ref. [25]. By properly adjusting the asymmetric factor λ, the peaks' height at the excited states can be quite large, again with small electrical and thermal conductances. As shown in Refs. [25] and [40], if the line-width function of the right colder electrode Γ_R is larger than Γ_L, the FOM will be suppressed, which is not shown here.

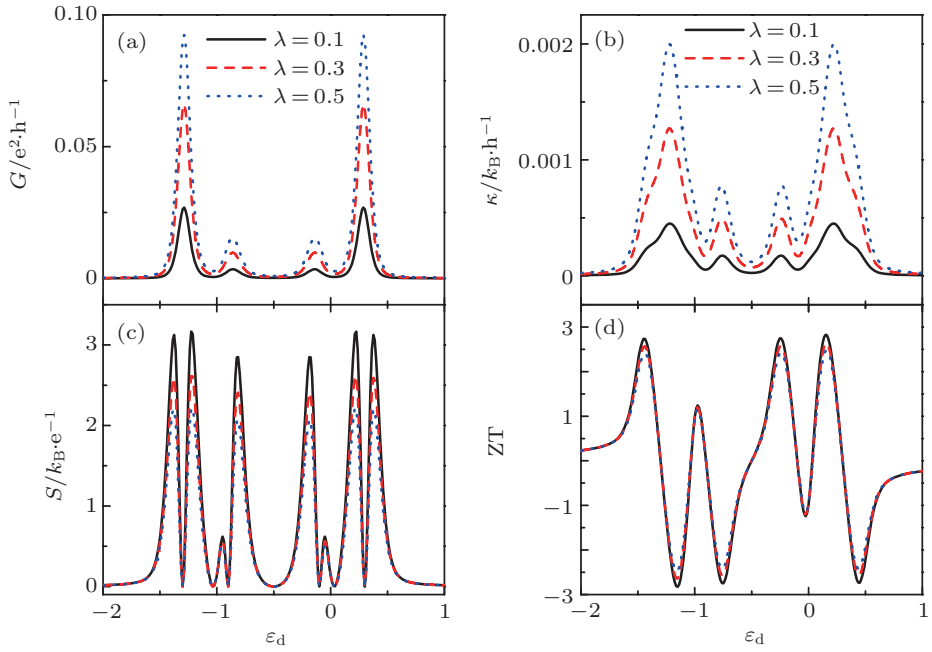


Fig. 3. (color online) (a) G, (b) κ, (c) S, and (c) ZT as functions of the dot level ε_d for $J = 0.4$ with different values of left–right coupling asymmetry $\lambda = \Gamma_R/\Gamma_L$ for $\Gamma_R = 0.02$ and $T = 0.03$.

Finally, we present in Fig. 4 the FOM as a function of the dot level for different values of operating temperature T. As is expected, the value of ZT will be enhanced with increasing temperature in the thermal energy region of $k_BT < U/10$. For $k_BT > U/10$,[16,24,25] the value of FOM will decrease with increasing temperature (not shown here). As compared to Fig. 2(d), the height difference between the twin peaks at the left and right sides of each molecular state is increased by

the increase in the temperature. The behavior of the FOM is again mainly determined by the non-monotonic dependence of the thermal conductance on the temperature.[16,24,25] In the present manuscript, we mainly focus on low-temperature regime, as did in most experiments regarding to QD. In Figs. 3 and 4, we only show the results for $J > 0$. If $J < 0$, the results are essentially the same and are not given here.

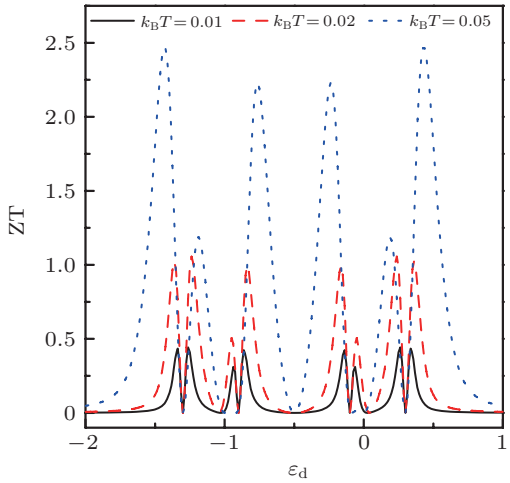


Fig. 4. (color online) Figure of merit as a function of the dot level for different values of the operating temperature T with $\Gamma_L = \Gamma_R = 0.02$ and $J = 0.4$. The behavior in the case of $J < 0$ resembles the present result (not shown in the figure).

4. Conclusion

In conclusion, impacts of exchange interaction between a magnetic impurity in a quantum dot and electrons entering into it on the thermoelectric effect are studied in the Coulomb blockade regime. We find a multiple-peak configuration in the physical quantities such as the electrical conductance, thermal conductance, thermopower, and figure of merit. The values of the electrical and thermal conductances will be visibly suppressed at the molecular states formed by the spin unpaired electron on the magnetic impurity and the electron entering the dot. The values of the thermopower and the figure of merit, however, can be as large as or a bit smaller than the case of the quantum dot system free from magnetic impurity. This enables the device to work at lower electrical and thermal conductance with high efficiency of converting heat into electricity, or vice versa. We find that the thermopwer and the figure of merit can be enhanced by properly adjusting the dot–electrode asymmetry and the operating temperature.

References

[1] Park H, Park J, Lim A K L, Anderson E H, Alivisatos A P and McEuen P L 2000 *Nature* **407** 57
[2] LeRoy B J, Lemay S G, Kong J and Dekker C 2001 *Nature* **432** 371
[3] Venkatasubramanian R, Siivola E, Colpitts T and O'Quinn B 2001 *Nature* **413** 597
[4] Hochbaum A I, Chen R, Delgado R D, Liang W, Garnett E C, Najarian M, Majumdar A and Yang P 2008 *Nature* **451** 163
[5] Blukai A I, Bunimovich Y, Tahir-Kheli J, Kan Y J, Goddard III W A and Heath J R 2008 *Nature* **451** 168
[6] Hicks L D and Dresselhaus M S 1993 *Phys. Rev. B* **47** 16631
[7] Kim T S and Hershfield S 2002 *Phys. Rev. Lett.* **88** 136601
[8] Humphrey T E and Linke H 2005 *Phys. Rev. Lett.* **94** 096601
[9] Finch C M, Garcia-Suarez C M and Lambert C J 2009 *Phys. Rev. B* **79** 033405
[10] Snyder G J and Toberer E S 2008 *Nat. Mater.* **7** 105
[11] Balandin A 2011 *Nat. Mater.* **10** 569
[12] Li N B, Ren J, Wang L, Zhang G, Hänggi P and Li B W 2012 *Rev. Mod. Phys.* **84** 1045
[13] Wang R Q and Jiang K M 2009 *Chin. Phys. B* **18** 5443
[14] Xiao X B, Li X M and Chen Y G 2009 *Chin. Phys. B* **18** 5462
[15] Bai X F, Chi F, Zheng J and Li Y N 2012 *Chin. Phys. B* **21** 077301
[16] Kuo D M T and Chang Y C 2010 *Phys. Rev. B* **81** 205321
[17] Guo Y, Qin J G, Ceng X Y and Gu B L 2003 *Chin. Phys. Lett.* **20** 1124
[18] Lu M W, Zhang L D and Yan X H 2003 *Chin. Phys. Lett.* **20** 124
[19] Huang L, You J Q, Yan X H and Wei S H 2002 *Chin. Phys. Lett.* **19** 1505
[20] Zhang Y M and Xiong S J 2003 *Chin. Phys. Lett.* **20** 2023
[21] Dubi Y and Di Ventra M 2009 *Phys. Rev. B* **79** 081302
[22] Swirkowicz R, Wierzbicki M and Barnaś J 2009 *Phys. Rev. B* **80** 195409
[23] Zhou J and Yang R 2010 *Phys. Rev. B* **82** 075324
[24] Liu J, Sun Q F and Xie X C 2010 *Phys. Rev. B* **81** 245323
[25] Chi F, Zheng J, Lu X D and Zhang K C 2011 *Phys. Lett. A* **375** 1352
[26] Kubala B, König J and Pekola J 2008 *Phys. Rev. Lett.* **100** 066801
[27] Wierzbicki M and Świrkowicz R 2011 *Phys. Rev. B* **84** 075410
[28] Liu Y S, Chi F, Yang X F and Feng J F 2011 *J. Appl. Phys.* **109** 053712
[29] Trocha P and Barnaś J 2012 *Phys. Rev. B* **85** 085408
[30] Gómez-Silva G, Ávalos-Ovando O, Ladrón de Guevara M L and Orellana P A 2012 *J. Appl. Phys.* **111** 053704
[31] Zheng J and Chi F 2012 *J. Appl. Phys.* **111** 093702
[32] Zheng J, Chi F and Guo Y 2012 *J. Phys.: Condens. Matter* **24** 265301
[33] Dong B and Lei X L 2002 *J. Phys.: Condens. Matter* **14** 11747
[34] Scheibner R, Buhmann H, Reuter D, Kiselev M N and Molenkamp L W 2005 *Phys. Rev. Lett.* **95** 176602
[35] Costi T A and Zlatić 2010 *Phys. Rev. B* **81** 235127
[36] Heersche H B, de Groot Z, Folk J A, Kouwenhoven L P, van der Zant H S J, Houck A A, Labaziewicz J and Chuang I L 2006 *Phys. Rev. Lett.* **96** 017205
[37] Tolea M and Bulka B R 2007 *Phys. Rev. B* **75** 125301
[38] Lu H Z and Shen S Q 2008 *Phys. Rev. B* **77** 235309
[39] Dubi Y and Di Ventra M 2011 *Rev. Mod. Phys.* **83** 131
[40] Zhu L C, Jiang X D, Zu X T and Lü H F 2010 *Phys. Lett. A* **374** 4269